

Entanglement and its evolution following a quench in the presence of an energy current

Anirban Das^{(1,2)*}, Silvano Garnerone^(2,3), and Stephan Haas^(1,2)

Departments of ⁽¹⁾Physics & Astronomy, and ⁽²⁾Center for Quantum Information Science & Technology, University of Southern California, Los Angeles, CA 90089, USA

⁽³⁾Institute for Quantum Computing, University of Waterloo, Waterloo, ON N2L 3G1, Canada

We study the Ising spin chain with a Dzyaloshinskii-Moriya interaction focusing on the static and dynamic properties of the entanglement entropy, following a quantum quench. We show that the effects of the additional anisotropic interaction on the phase diagram and on the dynamics of the system are captured by the properties of the entanglement entropy. In particular, the model provides a way to study the quench dynamics in a system with an energy current. We consider quenches starting from an initial excited state of the Ising spin chain, and we analyze the effects of different initial conditions.

I. INTRODUCTION

Recent experiments have shown that it is possible to study unitary nonequilibrium dynamics in quantum systems on long time scales [1]. One important result of these investigations has been the observed lack of thermalization. The reason for this non-thermal behaviour is attributed to the near integrability of the system. This observation has motivated recent studies of the non-equilibrium properties of integrable quantum model Hamiltonians [2]. The interest in this topic is also motivated by its relevance to a variety of experimental situations, including cold atoms [3], Penning traps [4] and Josephson-junction arrays [5].

There are many ways in which it is possible to drive a system out of equilibrium. Quantum quenches, and coupling to baths with different temperatures (or potentials) are the most common protocols. While in the quench scenario the focus is on the unitary dynamics of the full system, in the second case one usually deals with an effective description of the dynamics of the subsystem only. Different out-of-equilibrium dynamics have nevertheless similar characteristics, for example the presence of currents (of particles, energy, or heat).

In this work, we study an Ising-like model system driven out of equilibrium with a quantum quench in the presence of an energy current. In the usual quench protocol the system is prepared in the ground-state in the absence of any current, and subsequently the dynamics drives it to some excited state. The model Hamiltonian we consider here allows for the study of two different new situations: a quench from the ground-state in the presence of an energy current, and a quench from an initial excited state in the absence of an energy current. The two scenarios are associated with different Hamiltonians which, in a sense, are dual to each other. To characterize the system's behaviour we focus our attention on the Entanglement Entropy (EE), as measured by the Von Neumann entropy, which is a central quantity in the characterization of nonequilibrium quantum dynamics [6].

The structure of the paper is the following: in Sec.II we introduce and describe the properties of the model Hamiltonian, in Sec.III we consider the static properties of EE for this model, and in Sec.IV we study the dynamics of entanglement

following a quench. Finally, we state our conclusions. In the Appendix the reader can find more details of the calculations.

II. THE MODEL

We consider an Ising spin chain in transverse field H_I , with an additional Dzyaloshinskii-Moriya (DM) interaction H_{DM} . The total Hamiltonian $H_I + H_{DM}$ is defined as follows

$$H = - \sum_j \left[\frac{1}{2} \sigma_j^x \sigma_{j+1}^x + \frac{h}{2} \sigma_j^z + \frac{\zeta}{8} (\sigma_j^x \sigma_{j+1}^y - \sigma_j^y \sigma_{j+1}^x) \right], \quad (1)$$

where h is the external magnetic field, and ζ is the coupling parameter determining the strength of the DM interaction. Such an anisotropic interaction is present in many low-dimensional materials with the necessary crystal symmetry, and it originates from spin-orbit coupling [7, 8]. Furthermore, the DM interaction is of relevance in quantum information theory, since it plays an important role in the physics of quantum dots [9], and in fault-tolerant quantum computation [10].

Adding the DM term to H_I does not affect the solvability of the model [11], and interestingly enough it provides the system with a richer phase diagram. These features have been used in [12] to study the effective out-of-equilibrium quantum dynamics of the model. H_{DM} can be viewed as a current term. The reason for this is the following. The equation of motion for the local energy density of H_I , defined by $\epsilon_j = \frac{1}{2} \sigma_j^x \sigma_{j+1}^x + \frac{h}{2} \sigma_j^z$,

$$\dot{\epsilon}_j = \frac{i}{\hbar} [H_I, \epsilon_j]. \quad (2)$$

One can write the time derivative of the energy current as the divergence of the energy current

$$\dot{\epsilon}_j = C_j - C_{j+1}, \quad (3)$$

with

$$C_j \propto \sigma_j^y (\sigma_{j-1}^x - \sigma_{j+1}^x). \quad (4)$$

It thus follows that H_{DM} is precisely the sum over all sites of the local currents $\sum_j C_j$. Therefore, the ground-state expectation value of H_{DM}

$$J \equiv \left\langle \sum_j \frac{\zeta}{8} (\sigma_j^x \sigma_{j+1}^y - \sigma_j^y \sigma_{j+1}^x) \right\rangle, \quad (5)$$

* anirband@usc.edu

becomes an order parameter indicating the presence of an energy current. Once the total Hamiltonian has been diagonalized, which can be done with the usual Jordan-Wigner and Bogoliubov transformations

$$H = \sum_q \Lambda_q b_q^\dagger b_q, \quad (6)$$

the effect of the DM interaction is clearly observed at the single-particle level. The single-particle spectrum is given by

$$\Lambda_q = \sqrt{1 + h^2 + 2h \cos q} + \zeta \sin q, \quad (7)$$

with $q \in [-\pi, \pi)$ the momentum of the quasi-particle. As can be seen in the above expression and in Fig.1, the DM interaction makes the spectrum non-symmetric with respect to $q = 0$. Note that the ground state of the Hamiltonian including the DM interaction is the same for all values of ζ in the interval $[0, 1]$. In particular this means that, within this range of values, the Ising model in a transverse field H_I and the system described by Eq.1 have the same ground state. Beyond $\zeta = 1$ (with $h \leq \zeta$) the Fermi sea starts to be populated by the modes in between the zeros of the single particle spectrum (i.e. between q_+ and q_- in Fig.1). This implies that the ground state is not anymore that of H_I . Furthermore, since the DM term commutes with the rest of the Hamiltonian, at the many-body level when $\zeta = 1$ we must have a level crossing between the ground state of H_I and some previously excited Hamiltonian eigenstates. Fig.2 shows the phase diagram of the model [12]. There are three regions: ferromagnetic, polarized paramagnetic, and the so-called current phase, characterized by $J \neq 0$. The current phase is gapless, and the two-point correlation functions show a power-law behaviour with an oscillatory amplitude: $\langle \sigma_i^x \sigma_{i+n}^x \rangle_{gs} \sim \frac{Q(h, \zeta)}{\sqrt{n}} \cos(kn)$, where Q is a non-universal function and $k \equiv \arccos \frac{1}{\zeta}$ [12].

In the following, we study the entanglement properties of this model, and subsequently we analyze new quench protocols for this spin system.

III. STATIC ENTANGLEMENT ENTROPY AND PHASE DIAGRAM

In this section we show how entanglement can be used to characterize the different phases of the model. To measure the EE, we consider a bipartition of the spin chain into two subsystems A and B. For this setup a good measure of EE between the two partitions is given by the von Neumann entropy $S_A \equiv -\text{Tr} \rho_L \ln \rho_L$, where ρ_L is the ground-state reduced density matrix of the subsystem A with L spins.

It is known that for critical one-dimensional systems the EE scales logarithmically in the subsystem size, with a prefactor given by the central charge of the associated Conformal Field Theory (CFT),

$$S_L = \frac{c}{3} \ln L + S_0, \quad (8)$$

where c is the central charge and S_0 is a non-universal constant [13, 14]. On the other hand, in the non-critical region

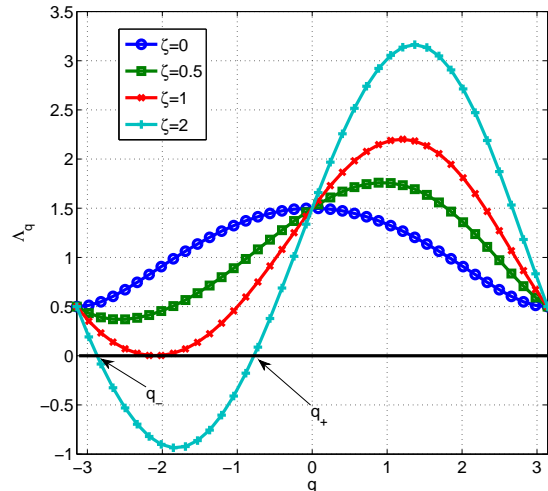


FIG. 1. (Color online) Spectrum of the Hamiltonian in Eq.1. We show the spectrum for 4 different values of ζ , while keeping $h = 0.5$ fixed. See also figures in [12].

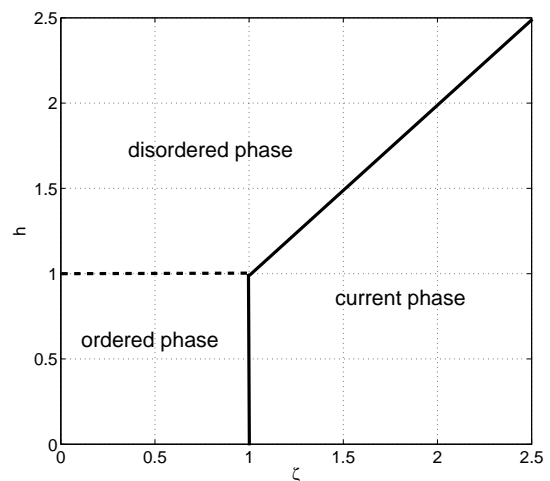


FIG. 2. (Color online) Phase diagram in the $h - \zeta$ plane of the model in Eq.1. The dotted line is a critical line where the model shows the same universal properties of the quantum Ising model in transverse field. See also figures in [12].

of the phase diagram, the entanglement entropy saturates to a value which depends on the correlation length ξ ,

$$S_L \propto \frac{c}{3} \ln \xi. \quad (9)$$

Both Eq.8 and Eq.9 characterize the ground-state properties of EE for one-dimensional systems.

Apart from the ground state it is also of interest to investigate entanglement properties of excited states. Recently, two works have appeared on this topic. In [15] it has been shown that there are excited states for which the logarithmic scaling of EE can have prefactors different from the ground state, and

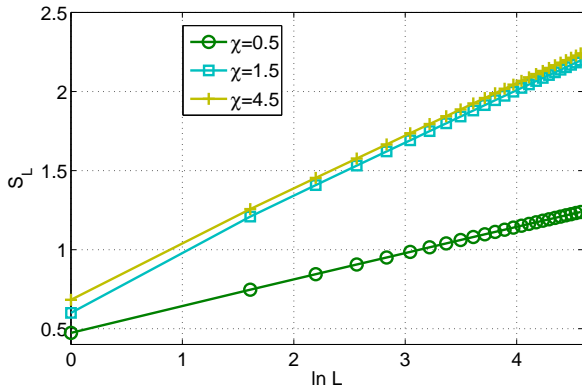


FIG. 3. (Color online) S_L vs L at $h = 1.0$ for different ζ . The scaling behavior changes from $S_L \sim \frac{1}{6} \ln L$ on the critical line separating the ordered and disordered phase to $S_L \sim \frac{1}{3} \ln L$ inside the current-carrying phase.

that for some excited states the scaling can be extensive in the subsystem size, instead of logarithmic. In [16] the authors have studied the connection between EE for excited states and properties of the associated CFT not contained in the central charge. The EE of excited states is of interest also in the context of quantum quenches since in this setting the system is unitarily driven from the initial ground state to an excited state.

The Hamiltonian in Eq.1 naturally fits in this set of problems. Following the discussion from the previous section the model we are considering allows us to study the EE of some excited states of H_I , simply by tuning the coupling constant associated with the DM term. The excitations we can consider in this way are characterized by the modes in between the zeros of the single particle spectrum that get populated when $\zeta > 1$ and $h < \zeta$ (7). For these states the EE can be evaluated analogously to the ground state of H_I (see also [17] for related analytical study).

Let us consider in detail the entanglement properties of the different phases shown in Fig.2. First, we compare the scaling of the entanglement in the non-current-carrying critical regions and in the region where an energy current is present. Fig.3 shows the result of the simulations for the scaling behaviour of the ground-state EE with $\zeta < 1$ and $h = 1$. For all values of $\zeta \in [0, 1]$ one observes the same scaling result. In the non-current-carrying region critical states are present only on the $h = 1$ line of the phase diagram. On this line, separating the ferromagnetic and polarized paramagnetic phases, the ground state of the system is the same as in H_I . This implies that the EE scaling is logarithmic with a prefactor of $c/3$, and $c = 1/2$. Note that also the entire current-carrying phase ($\zeta > 1$ and $h < \zeta$) is gapless, and in this sense critical. At any point in this phase we observe logarithmic scaling of the EE in the subsystem size. This is consistent with the discussion in the previous section on the algebraic decay of the two point correlation function. Interestingly, the prefactor of the logarithmic scaling of EE in the current phase is twice as large as the prefactor in the non-current phase. This doubling reflects

the increased number of zeros in the single-particle spectrum, consistent with the results of [17]. In fact, when $\zeta > 1$ the ground state of Eq.1 is the filled Fermi sea of modes in between q_- and q_+ (see Fig.1). Since the ground-state in the current phase is effectively an excited eigenstate of H_I , we could expect a scaling of EE that is extensive in the system size, as shown in [15] for excited states. The reason why this is not the case is due to the nature of the single-particle spectrum, which at most can have two zeros (see Fig.1), and thus does not satisfy the requirements found in [15] for an extensive scaling of EE.

The DM interaction in the Hamiltonian affects also the sub-leading term in the scaling of EE $S_L = \frac{1}{3} \ln L + S_0(h, \zeta)$. Deriving the analytical form of the sub-leading order term $S_0(h, \zeta)$ is complicated. Nonetheless, one can investigate this term numerically. In Fig.4 we see that S_0 is constant on the critical line $h = 1$ with $\zeta \leq 1$. As soon as $\zeta > 1$ and $h < \zeta$, S_0 increases, but becomes almost constant for large ζ . Also S_0 is maximum at $h = 0$, and S_0 is minimum at the critical point $h = \zeta$. From the behaviour of S_0 we can conclude that a given block has the highest entanglement when all the negative modes ($q \in [-\pi, 0)$) in the Fermi sea are filled. Consequently EE increases with higher values of the energy current.

We now consider the differences between the critical lines shown in the phase diagram (Fig.2), separating different phases. The only second-order quantum phase transition is found along at the $h = 1$ line (with $\zeta \leq 1$), which corresponds to the Ising quantum phase transition (see Fig. 5). On the hand the boundaries of the current-carrying phase with both the paramagnetic and the ferromagnetic phases are characterized by a level crossing. This translates into a sudden jump in EE (see Fig.5 and Fig.6). The value of EE is always higher in the current carrying phase because of the presence of long-range correlations that decay algebraically. The plots in Fig.5 and Fig.6 show that controlling the DM term can be used as an entanglement switch. The amount of entanglement can be driven by the DM coupling term or the magnetic field, which are controllable parameters in optical lattices [18].

IV. ENTANGLEMENT DYNAMICS FOLLOWING A QUENCH

In this section, we focus on the quench dynamics of the EE. Quenching provides a way to excite a system, initially prepared in the ground state, and to subsequently study the non-equilibrium dynamics of the model (in the following, we denote with a subscript 0 the value of the parameters describing the initial Hamiltonian). As stated previously, the model in Eq.1 is of interest because it combines two different mechanisms typically used to drive a system out of equilibrium: quantum quenching, and the coupling to a field originating a current in the system. Furthermore the inclusion of the DM term allows us to study a model Hamiltonian where the energy current can be controlled and used in the quench protocol.

In our setup, the quench can either involve the magnetic field h , the DM coupling ζ or a combination of the two. Since the DM term commutes with the Hamiltonian, a quench in ζ

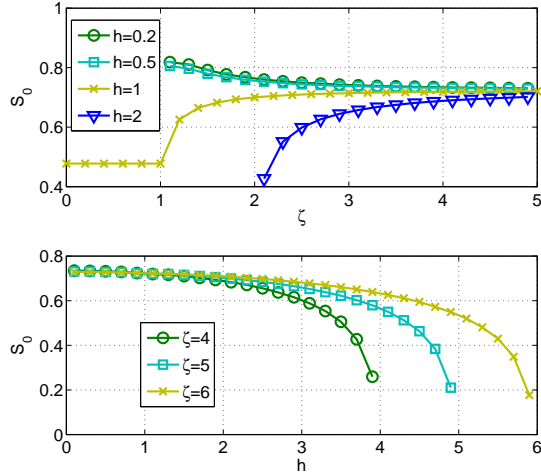


FIG. 4. (Color online) Non-universal nature of S_0 . (upper panel) S_0 vs. ζ at different h ; (lower panel) S_0 vs. h at different ζ .

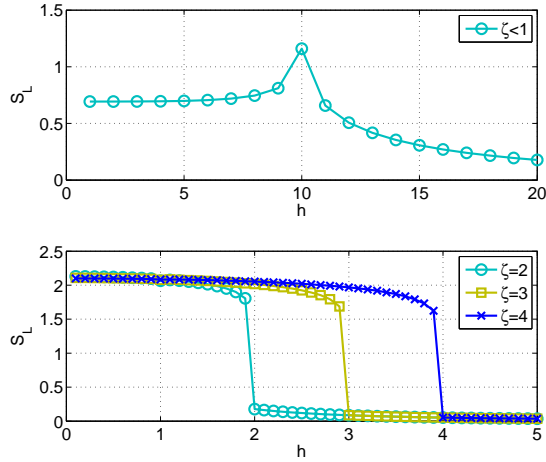


FIG. 5. (Color online) S_L vs. h at $L = 60$ for different ζ . (upper panel) Static entanglement along the transition between the ordered ferromagnetic and the disordered paramagnetic phase. The peak signals the presence of long-range correlations at the critical point, which is a signature of a second-order quantum phase transition. (lower panel) Static entanglement along the transition between the disordered paramagnetic and the current-carrying phase. The sudden change in entanglement followed by the absence of a peak at the critical point is a signature of the first-order quantum phase transition.

leaves the system in one of its eigenstates, providing a trivial evolution of the EE. On the other hand, quenches in the magnetic field give more interesting behaviours. If the quench is done with the initial state prepared in a region with no current the results are similar to those found in [6], where quenches for the H_I were considered. This is due to the fact that, in the absence of a current, the ground-state wave function initially is identical to that of H_I , and the time evolution is not

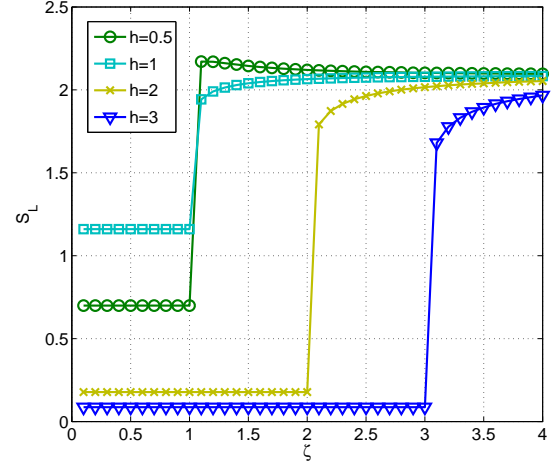


FIG. 6. (Color online) S_L vs. ζ at $L = 60$ for different h . The plots for $h = 0.5$ corresponds to the static entanglement along the transition between the ordered ferromagnetic and the current-carrying phase. This is a first order quantum phase transition which occurs at $\zeta = 1$ (analogously for $h = 1$). The plots for $h = 2$ and $h = 3$ correspond to the static entanglement along the transition between the disordered and the current-carrying phase. This is a first order QPT which occurs at $\zeta = h$.

affected by the presence of the DM term (see the derivation of Eq.25 in the Appendix for a proof of this). More interestingly, if the quench involves an initial state inside the current phase, new non-trivial behaviours can be expected, since the ground state now is radically different. It is important to notice that the DM coupling enters only in the specification of the initial state, whereas the evolution can be effectively described by the Hamiltonian without the DM term. The calculations showing that this is in fact the case can be found in the Appendix.

We first compare the evolution of the EE for different quenches inside the current-carrying phase. Fixing the coupling constant of the DM term, and quenching only the external magnetic field we obtain the results shown in Fig.7. One always has an initial ballistic evolution of the EE, which grows linearly in time (measured in units where the speed of the elementary excitation is unity) and saturates at some point. Quite interestingly, the saturation time (hence also the rate at which entanglement is initially building up) depends on the particular evolving Hamiltonian. This way we can control the time needed to generate the maximal asymptotic amount of entanglement. This property is relevant also from a computational point of view. In fact, DMRG-like schemes, used for the simulation of the time evolution of quantum systems, can take advantage of the lower rate at which entanglement is generated. Knowing the regions in the phase diagram where such rates are lower can provide more efficient time simulations. As far as we know this is a new feature that is not present in other quench protocols considered so far in the literature. The other aspect that is important to notice in Fig.7 is the special role played by the line $h = 1$ in the phase diagram, which

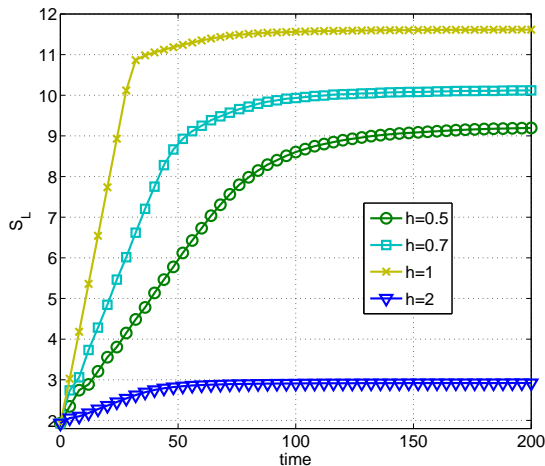


FIG. 7. (Color online) Quenches from the current carrying phase. $S_L(t)$ vs. the time steps, with $L = 60$, $h_0 = 4.0$, $\zeta_0 = \zeta = 5.0$ for different h . Note that the extent of the initial linear regime depends on the particular evolving Hamiltonian.

turns out to provide the maximum asymptotic EE for different quench parameters. This can be understood by mapping the quench for $H_I + H_{DM}$ to a quench protocol for H_I only. As stated in the previous section, the entanglement evolution with respect to $H(h, \zeta)$ is identical to the evolution with respect to $H(h, 0)$. Furthermore, the ground state of $H(h_0, \zeta_0)$, the initial Hamiltonian in the quench protocol is also an excited eigenstate of $H(h_0, 0)$, because of the commutativity of the DM term with the total Hamiltonian. From this dual perspective the effect of the current is that of effectively quenching an excited eigenstate without the current term. For the Ising model, a quench from $h_0 \neq 1$ yields the maximum value of $S_L(\infty)$ when quenched to $h = 1$, because the energy gap closes at $h = 1$, and hence a large number of zero energy excitations can be produced. While the asymptotic value of EE depends on the particular excited state at the beginning of the quench.

Fig.8 shows results of simulations for quenches with increasing values of the DM field in the current-carrying phase. The asymptotic value of the EE decreases with increasing ζ . This is consistent with the phenomenological picture provided in [6], and with the fact that if the system starts in an excited state, the available number of unoccupied modes that can be occupied after the quench is smaller than in the case of having the ground state as an initial state. Furthermore, Fig.8 shows that the time at which the EE saturates does not depend on ζ , and consequently does not depend on the particular initial Hamiltonian eigenstates (as long as it is not an eigenstate of the evolving Hamiltonian). The line with $\zeta = 100$ in Fig.8 shows that very deep into the current phase quenching does not create entanglement. In fact, when $\zeta \gg h_0$ quenching the magnetic field is just a small perturbation to the Hamiltonian, which then approximately stays in the ground state.

Finally, we verify that the presence of an energy current does not affect the extensive nature of the asymptotic value

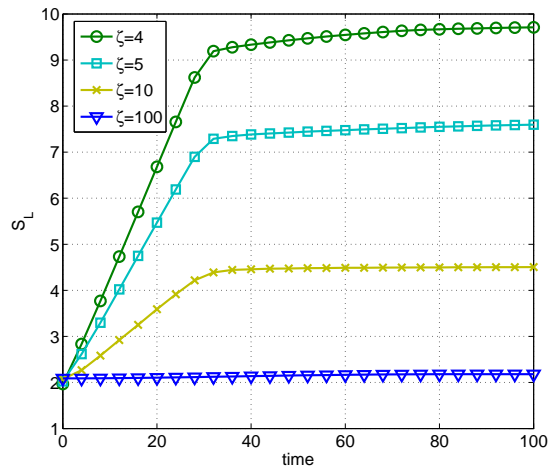


FIG. 8. (Color online) Quenches from the current carrying-phase with different values of the current driving field ζ . $S_L(t)$ vs. the time steps with $L = 60$, $h_0 = 3.0$ to $h = 1$ for different $\zeta_0 = \zeta$.

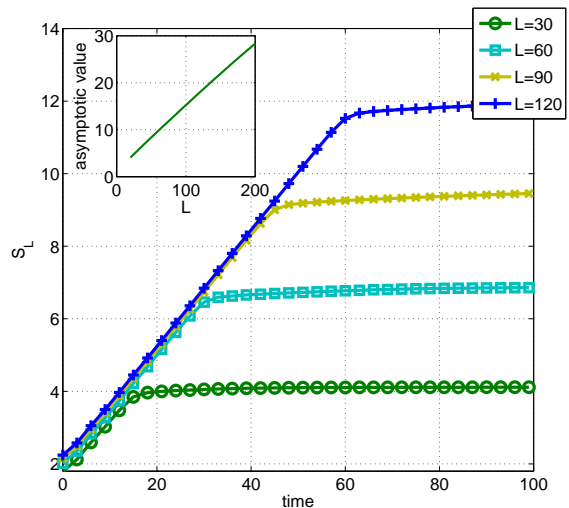


FIG. 9. (Color online) $S_L(t)$ vs. the time steps inside the current-carrying phase for different block sizes L . Quenching is done from $h_0 = 2.0$ to $h = 1.0$ with $\zeta_0 = \zeta = 3.0$.

of EE (Fig.9), and its proportionality with the quench size (Fig.10).

V. CONCLUSIONS

We have studied the static and dynamic properties of the entanglement entropy in the Ising spin chain with a transverse field and a Dzyaloshinskii-Moriya interaction. The model is characterized by the presence of an energy current for certain regions of the phase diagram.

Concerning the static properties we have analyzed the transitions between phases with no energy current and the phase

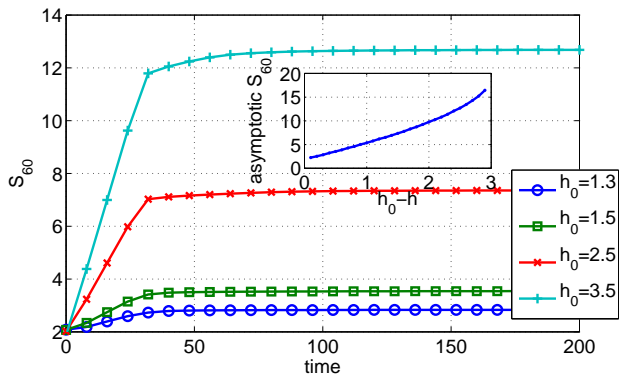


FIG. 10. (Color online) $S_{60}(t)$ vs. the time steps for quenches to $h = 1$ from various h_0 inside the current-carrying phase at $\zeta = \zeta_0 = 4$.

where an energy current is present. The transition is captured by a discontinuity of EE as a function of the parameters, and by a distinguishable scaling behaviour in the current-carrying and non-current-carrying regions. In particular, the leading logarithmic term of the EE scaling with respect to the system size has a prefactor in the current-carrying region which is twice as large compared to the second order Ising critical line.

Concerning the behaviour of the entanglement evolution following a quench, the model in Eq.1 allows us to study new

quench protocols. The usual schemes consider quenches from an initial ground state. This scenario, for the model in Eq. 1, effectively corresponds to a quench from an initially excited state of the Ising spin chain in transverse field (without DM interaction). The main result of this analysis shows that the ballistic picture presented in [6] is still valid, although with a significantly different aspect. In particular the entanglement saturation time in the current-carrying phase depends on the details of the evolving Hamiltonian. This is an indication of the role played by the evolving Hamiltonian on the propagation of excitations. This result is of relevance in tuning the dynamics of the system in regions with a different rate for the propagation of entanglement. Furthermore it also provides a characterization of the regions in the phase diagram that can be simulated more efficiently with DMRG-like techniques.

From a general point of view, the model in Eq. 1 also suggests a simple way to study the quench dynamics of initial excited states in integrable systems. The addition of a commuting term in the Hamiltonian causes a reshuffling of the spectrum that, without changing the integrability of the model, allows us to obtain non-trivial results about the excitations in the original model. The same trick can be applied to other systems of interest.

We thank Letian Ding, Zoltan Racz, and Paolo Zanardi for useful comments. This work has been supported by NSF grants PHY-803304, and DMR-0804914.

-
- [1] M. Greiner et al., *Nature* **419**, 51 (2002); T. Kinoshita, T. Wenger and D. S. Weiss, *Nature* **440**, 900 (2006); S. Hofferberth et al., *Nature* **449**, 324 (2007); S. Trotzky et al., arXiv:1101.2659.
- [2] A. C. Cassidy, C. W. Clark, and M. Rigol, *Phys. Rev. Lett.* **106**, 140405 (2011); M. Rigol, *Phys. Rev. Lett.* **103**, 100403 (2009); M. Rigol, V. Dunjko, V. Yurovsky, and M. Olshanii, *Phys. Rev. Lett.* **98**, 050405 (2007); P. Calabrese, and J. Cardy, *Phys. Rev. Lett.* **96**, 136801 (2006); S. R. Manmana, S. Wessel, R. M. Noack, and A. Muramatsu, *Phys. Rev. Lett.* **98**, 210405 (2007);
- [3] I. Bloch, J. Dalibard, and W. Zwerger, *Rev. Mod. Phys.* **80**, 885964 (2008).
- [4] G. Ciaramicoli, I. Marzoli, and P. Tombesi, *Phys. Rev. A* **78**, 012338 (2008).
- [5] Y. Makhlin, G. Schon, and A. Shnirman, *Rev. Mod. Phys.* **73**, 357400 (2001).
- [6] P. Calabrese and J. Cardy, *J. Stat. Mech.* P06002 (2004).
- [7] I. Dzyaloshinskii, *Phys. Chem. Solids* **4**, 241 (1958); T. Moriya, *Phys. Rev.* **120**, 91 (1960).
- [8] M. Oshikawa and I. Affleck, *Phys. Rev. Lett.* **79**, 2883 (1997); J. Z. Zhao, X. Q. Wang, T. Xiang, Z. B. Su, and L. Yu, *Phys. Rev. Lett.* **90**, 207204 (2003); I. Tsukada, J. Takeya, T. Masuda, and K. Uchinokura, *Phys. Rev. Lett.* **87**, 127203 (2001); S. Bertaina, V. A. Pashchenko, A. Stepanov, T. Masuda, and K. Uchinokura, *Phys. Rev. Lett.* **92**, 057203 (2004); M. Kohgi, K. Iwasa, J.-M. Mignot, B. Fak, P. Gegenwart, M. Lang, A. Ochiai, H. Aoki, and T. Suzuki, *Phys. Rev. Lett.* **86**, 2439 (2001).
- [9] S. Chutia, M. Friesen, and R. Joynt, *Phys. Rev. B* **73**, 241304(R) (2006).
- [10] L. A. Wu and D. A. Lidar, *Phys. Rev. Lett.* **91**, 097904 (2003).
- [11] Th. J. Siskens, H. W. Capel, and K. J. F. Gaemers, *Physica A* **79**, 259 (1975).
- [12] T. Antal, Z. Racz, and L. Sasvari, *Phys. Rev. Lett.* **78**, 167 (1997).
- [13] L. Amico, R. Fazio, A. Osterloh, and V. Vedral, *Rev. Mod. Phys.* **80**, 517 (2008).
- [14] G. Vidal, J. I. Latorre, E. Rico, and A. Kitaev, *Phys. Rev. Lett.* **90**, 227902 (2003).
- [15] Vincenzo Alba, Maurizio Fagotti, Pasquale Calabrese, *Journal of Stat. Mech.* P10020 (2009).
- [16] F. C. Alcaraz, M. I. Berganza, and G. Sierra, *Phys. Rev. Lett.* **106**, 201601 (2011).
- [17] Z. Kadar and Z. Zimboras, *Phys. Rev. A* **82**, 032334 (2010); J. P. Keating, and F. Mezzadri, *Commun. Math. Phys.*, **252** 543 (2004); V. Eisler, and Z. Zimboras, *Phys. Rev. A* **71**, 042318 (2005).
- [18] M. Greiner et al., *Nature* **472**, 307 (2011);
- [19] K. Sengupta, S. Powell, and S. Sachdev, *Phys. Rev. A* **69**, 053616 (2004).

Appendix. In this Appendix we give a detailed description of the steps involved in first evaluating the entanglement entropy of the Hamiltonian in Eq.1, and then calculating its time evolution. After the standard sequence of Jordan-Wigner and Bogoliubov transformations the Hamiltonian is in the diagonal form $H = \sum_{k=-\pi}^{\pi} \Lambda_k b_k^\dagger b_k$, with $\Lambda_k = \frac{1}{2}(\sqrt{1 + h^2 + 2h \cos k} + \zeta \sin k)$. The density matrix of the subsystem of size L, embedded in

a system of size N , can be obtained tracing out the rest of the system

$$\rho_L = \text{Tr}_{N-L}(\rho) = A_0 e^{-\mathcal{H}}, \quad (10)$$

where A_0 is a normalization constant and \mathcal{H} is a quadratic hermitian operator

$$\mathcal{H} = \sum_{i,j=1}^L c_i^\dagger V_{i,j} c_j + \frac{1}{2} (c_i^\dagger W_{i,j} c_j^\dagger - c_i W_{i,j} c_j). \quad (11)$$

\mathcal{H} can be diagonalized via a generalized Bogoliubov transformation. The reduced density matrix has the form

$$\rho_L = A_0 \exp\left[-\sum_{q=1}^L \varepsilon_q d_q^\dagger d_q\right] \quad (12)$$

Using $\text{Tr}(\rho_L) = 1$, we get $A_0 = \prod_{q=1}^L \frac{1}{1 + \exp(-\varepsilon_q)}$. This gives the final form of the density matrix as

$$\rho_L = \prod_{q=1}^L \frac{\exp(-\varepsilon_q d_q^\dagger d_q)}{1 + \exp(-\varepsilon_q)}. \quad (13)$$

Defining $\nu_q \equiv \frac{1 - \exp(-\varepsilon_q)}{1 + \exp(-\varepsilon_q)}$, we can write

$$\rho_q \equiv \left(\begin{array}{cc} \frac{1 + \nu_q}{2} & 0 \\ 0 & \frac{1 - \nu_q}{2} \end{array} \right), \quad (14)$$

and also

$$\begin{aligned} \rho_L &= \prod_{q=1}^L \frac{1 + \nu_q}{2} \exp\left[-\ln\left(\frac{1 + \nu_q}{1 - \nu_q}\right) d_q^\dagger d_q\right] \\ &= \prod_{q=1}^L \left(\frac{1 + \nu_q}{2} - \nu_q d_q^\dagger d_q\right) \\ &= \bigotimes_{q=1}^L \rho_q. \end{aligned} \quad (15)$$

Using the fact that $\exp(d_q^\dagger d_q \ln \lambda) = 1 + (1 - \lambda) d_q^\dagger d_q$, one has for the entanglement entropy

$$\begin{aligned} S_L &= -\text{Tr}(\rho_L \ln(\rho_L)) \\ &= \sum_{q=1}^L \left[\ln(1 + \exp(-\varepsilon_q)) + \frac{\varepsilon_q}{1 + \exp(\varepsilon_q)} \right] \\ &= -\sum_{q=1}^L \left(\frac{1 + \nu_q}{2} \ln \frac{1 + \nu_q}{2} + \frac{1 - \nu_q}{2} \ln \frac{1 - \nu_q}{2} \right). \end{aligned} \quad (16)$$

We have to calculate ν_q , from which we can obtain the block entropy. ν_q is given by the expectation value of $d_q^\dagger d_q$ and $d_q d_q^\dagger$

$$\begin{aligned} \langle d_q^\dagger d_q \rangle &= \text{Tr}(\rho_L d_q^\dagger d_q) = \frac{\exp(-\varepsilon_q)}{1 + \exp(-\varepsilon_q)} = \frac{1 - \nu_q}{2} \\ \langle d_q d_q^\dagger \rangle &= \text{Tr}(\rho_L d_q d_q^\dagger) = \frac{1}{1 + \exp(-\varepsilon_q)} = \frac{1 + \nu_q}{2}. \end{aligned} \quad (17)$$

We define four $2L \times 1$ column vector: $D \equiv \begin{pmatrix} d \\ d^\dagger \end{pmatrix}$, $C \equiv \begin{pmatrix} c \\ c^\dagger \end{pmatrix}$, $\bar{D} \equiv \begin{pmatrix} d^\dagger \\ d \end{pmatrix}$ and $\bar{C} \equiv \begin{pmatrix} c^\dagger \\ c \end{pmatrix}$, where $d = (d_1, \dots, d_L)^t$, and similarly for c . The previous Bogoliubov transformations can be expressed in a compact matrix notation as

$$D = \begin{pmatrix} g & h \\ h & g \end{pmatrix} C, \quad (18)$$

and

$$\bar{D}^t = \bar{C}^t \begin{pmatrix} g^t & h^t \\ h^t & g^t \end{pmatrix}, \quad (19)$$

where g and h are $L \times L$ matrices. In terms of expectation values we have

$$\langle D \bar{D}^t \rangle = \begin{pmatrix} g & h \\ h & g \end{pmatrix} \langle C \bar{C}^t \rangle \begin{pmatrix} g^t & h^t \\ h^t & g^t \end{pmatrix}. \quad (20)$$

Let us now consider a quantum quench protocol. Initially the system is prepared in the ground state of an Hamiltonian H' , and suddenly one of the parameters is changed, and the new Hamiltonian is denoted by H . The quasi-particle operator vector $B'_k \equiv (b'_k, b'^{\dagger}_{-k})^t$ is associated with H' , and the vector $B_k \equiv (b_k, b^{\dagger}_{-k})^t$ is associated with H . Similarly for C_k , which is associated with bare vacuum fermions. Define also the matrix $R_\mu(\alpha) \equiv \cos(\frac{\alpha}{2})\mathbb{I} + i\sigma_\mu \sin(\frac{\alpha}{2})$, where σ_μ are the Pauli matrices, and $\mu = x, y, z$. It can be easily seen that $C_k = R_x(\theta_k) B_k$, and $C_k = R_x(\theta'_k) B'_k$, with θ_k a parameter of the Bogoliubov transformation [19]. From which we can write $B_k = R_x(\theta'_k - \theta_k) B'_k$.

When a quench takes place, the time evolution of the fermion operators is given by $B_k(t) = e^{-iHt} B_k e^{iHt}$. We can write $B_k(t) = S_z(-2\Lambda_k t) B_k$, where

$$S_z(-2\Lambda_k t) = \begin{pmatrix} e^{-i\Lambda_k t} & 0 \\ 0 & e^{-i\Lambda_{-k} t} \end{pmatrix}.$$

Notice that the energy spectrum of the Hamiltonian in Eq.1 is not symmetric, which means that in general $\Lambda_{-k} \neq \Lambda_k$. In order to evaluate the two-point correlation functions we consider different cases. When the initial state of the system is in the non-current-carrying region we have

$$\langle B'_k B'_k{}^\dagger \rangle = \begin{pmatrix} 1 & 0 \\ 0 & 0 \end{pmatrix}. \quad (21)$$

If the initial state of the system is in the current-carrying phase and $k \in (k_1, k_2)$, where k_1 and k_2 are the zeros of the spectrum then

$$\langle B'_k B'_k{}^\dagger \rangle = \begin{pmatrix} 0 & 0 \\ 0 & 0 \end{pmatrix}. \quad (22)$$

For k lying between $-k_1$ and $-k_2$ we have

$$\langle B'_k B'_k{}^\dagger \rangle = \begin{pmatrix} 1 & 0 \\ 0 & 1 \end{pmatrix}. \quad (23)$$

A compact way of expressing Eq.21, Eq.22, and Eq.23 is given by

$$\langle B'_k B'_k{}^\dagger \rangle = \begin{pmatrix} \frac{1}{2}(1 + \frac{|\Lambda_k|}{\Lambda_k}) & 0 \\ 0 & \frac{1}{2}(1 - \frac{|\Lambda_{-k}|}{\Lambda_{-k}}) \end{pmatrix}. \quad (24)$$

Finally we can write

$$\begin{aligned} \langle C_k(t) C_k^\dagger(t) \rangle &= R_x(\theta_k) \langle B_k(t) B_k^\dagger(t) \rangle R_x^\dagger(\theta_k) \\ &= R_x(\theta_k) S_z(-2\Lambda_k t) \langle B_k B_k^\dagger \rangle S_z^\dagger(-2\Lambda_k t) R_x^\dagger(\theta_k) \\ &= R_x(\theta_k) S_z(-2\Lambda_k t) R_x(\theta'_k - \theta_k) \langle B'_k B'_k{}^\dagger \rangle \\ &\times R_x^\dagger(\theta'_k - \theta_k) S_z^\dagger(-2\Lambda_k t) R_x^\dagger(\theta_k). \end{aligned} \quad (25)$$

Notice that the above expression is the same if we consider $S_z(-2\Lambda_k t)$, with Λ_k the single particle spectrum of Eq.1, or if

we consider $S_z(-2\Lambda_k t)$, with Λ_k the single particle spectrum of the Ising Hamiltonian without the DM term. This can be seen with a direct calculation. For example, one entry of the above correlation matrix is given by

$$\begin{aligned} 2\langle c_{-k}^\dagger(t) c_{-k}(t) \rangle &= \\ E_1 + E_2 + (E_2 - E_1) \cos \theta_k \cos(\theta'_k - \theta_k) \\ + (E_1 - E_2) \cos[t(\Lambda_k + \Lambda_{-k})] \sin \theta_k \sin(\theta'_k - \theta_k), \end{aligned} \quad (26)$$

where $E_1 \equiv \frac{1}{2}(1 + \frac{|\Lambda_k|}{\Lambda_k})$ and $E_2 \equiv \frac{1}{2}(1 - \frac{|\Lambda_{-k}|}{\Lambda_{-k}})$. The argument of S_z appears only in the argument of the trigonometric function in such a way that the DM contribution is irrelevant (see Eq.7). This proves that the time evolution of the correlation matrix in Eq.25, with respect to the ground-state of Eq.1, is the same as the time evolution of the correlation matrix with respect to the Ising Hamiltonian in transverse field, with respect to an excited state of the Ising Hamiltonian.